

# An Introduction to Breakdown Phenomena in Disordered Systems

Rava da Silveira

Department of Physics, Massachusetts Institute of Technology, Cambridge, MA 02139

The rupture of a medium under stress typifies breakdown phenomena. More generally, the latter encompass the dynamics of systems of many interacting elements governed by the interplay of a driving force with a pinning disorder, resulting in a macroscopic transition. A simple mean-field formalism incorporating these features is presented and applied to systems representative of fracture phenomena, social dilemmas, and magnets out of equilibrium. The similarities and differences in the corresponding mathematical structures are emphasized. The solutions are best obtained from a graphical method, from which very general conclusions may be drawn. In particular, the various classes of disorder distribution are treated without reference to a particular analytical or numerical form, and are found to lead to qualitatively different transitions. Finally, the notion of effective (or phenomenological) theory is introduced and illustrated for non-equilibrium disordered magnets.

## I. INTRODUCTION

When boarding passengers, airline personnel usually call a limited number of rows at a time — “Now seating rows 20 to 30!” — to ensure an efficient and orderly filling of the aircraft. Nevertheless, there are always some hurried individuals who unduly join the forming line before their row is called, only to be rebuked by the flight attendant. In most instances the line is barely disrupted, while in some cases, such as delayed flights, the “avalanching” of disobedient passengers creates a long, disorderly line, absorbing nearly everyone. Why is this? Let us consider the mechanism by which the line forms in greater detail. First, the forty or so passengers whose rows have been called move toward the gate, initiating a line. Next, a few “impatiens” (or “disobedients”) add to the ranks, and perhaps also some absent-minded physicists who stand up as soon as they hear an announcement and innocently approach the gate. Seeing this, some of the people still sitting and waiting calmly, might lose their patience and decide to join the growing line. This “domino effect” may die out very soon, with just a few outsiders hiding in the queue, or it may continue, resulting in a catastrophic boarding process.

The line formation at a boarding gate incorporates all the elements of a *breakdown phenomenon* [1]: it involves a large number of elements (individuals), each in one of several possible states (sitting or in line), which interact (the longer the line, the stronger the temptation), and are driven as a whole (calls of the flight attendant). Furthermore, different people have different “obedience thresholds” that depend on their personality, mood, schedule, etc. For a given length of the line, a fraction of these thresholds are crossed and the resulting disobedients stand up and move toward the gate. Equivalently, a sitting individual decides to stand up and join the queue with some probability (dependent on the line’s length), thereby introducing an element of stochasticity, or *disorder*. Similar features are present in a great variety of processes, occurring, for example, in materials under tension [2–4], conductors with an imposed current [1,5], magnets driven by an applied field [6], and social phenomena such as the “boarding-gate problem.” The rupture of the material, destruction of the conductor, macroscopic flipping of the magnetization, or the failure of the social process, respectively, can be viewed as a breakdown of the system.

The present paper aims to draw a simple quantitative picture of breakdown phenomena in disordered systems, unifying the various realizations into a single formalism while still allowing for the details that distinguish each case. The most drastic simplification underlying our approach is its “mean-field” nature, which relies on average quantities by ignoring fluctuations and, consequently, any idea of locality or modulated spatial correlation. Although such a crude description can depart significantly from three-dimensional reality, it is often accurate in higher dimensions and establishes a coarse framework which may then be refined to include fluctuations (perturbatively). Nevertheless, some systems, such as magnets with long-range interactions or the boarding-gate line, are properly described by a mean-field theory; in the boarding gate problem, for example, any notion of locality is absent from the interactions, as any passenger can see the line as well as any other.

In addition to differences intrinsic to various examples, our approach should allow for the introduction of more than one type of disorder, as even a given system’s behavior might very well depend on the character of the stochasticity present. Better, we would like to divide all the possible disorder distributions into classes, each associated with a distinct qualitative behavior. To achieve this, we use a graphical scheme [3,4] where we can *draw* different disorder distributions, enabling us to handle the latter in a very general fashion, without reference to a particular analytical or numerical form, and to distinguish the features relevant to the breakdown phenomenon [4]. These features define the various “universality classes,” identified by one of their (drawn) members or by a generic statement (for example, “the class of all *continuous* distributions”). A graphical method also avoids the possible misconceptions of a more specific

treatment [7]. Indeed, if the qualitative behavior of a physical system changes upon making a particular, for example, Gaussian, distribution wider, what is the associated key feature? Is it the variance of the Gaussian or its maximum value? Finally, a graphical scheme allows us to “follow” the state of the system as it is driven, thus capturing the whole breakdown phenomenon in a single picture.

We develop the method in the context of fractures (Sec. II), for which it was originally devised [2,4], before applying it to two other realizations interesting in their own right. In Sec. III, some quantitative results are obtained for the boarding gate problem. Section IV focuses on driven magnets, a workhorse of non-equilibrium statistical mechanics as well as a central model for hysteresis. In Sec. V, we introduce the notion of effective (or phenomenological) theory, a broader framework than the models examined. We return to the discussion of driven magnets in this more general context by constructing a simple effective theory suited to the problem, and mention some natural extensions to richer, non-mean-field approaches. Finally, we conclude (Sec. VI) with a summarizing picture and a brief allusion to dynamics.

## II. FRACTURES AND EARTHQUAKES: THE DEMOCRATIC FIBER BUNDLE MODEL

The democratic fiber bundle model was introduced by Peirce [2] in 1926, and formalized and studied in greater detail by Daniels [3] in 1945. It consists of  $N_0$  ( $\rightarrow \infty$ ) fibers pulled by a force  $F$  which they share uniformly (democratically). As the force is increased, a fiber breaks if the stress it undergoes exceeds a threshold (or strength), drawn from a distribution  $p(x)$ . After each set of failures, the total force is redistributed over the remaining fibers. As members of the *British Cotton Industry Research Association* and the *Wool Industries Research Association*, respectively, Peirce and Daniels sought a more fundamental understanding of the ‘hank’ and ‘lea’ tests for wool and cotton yarns, in which a hank (or bundle) is stretched between two hooks until it ruptures. A more life-threatening illustration of the model is offered by the failure of an elevator rope (Fig. 1).

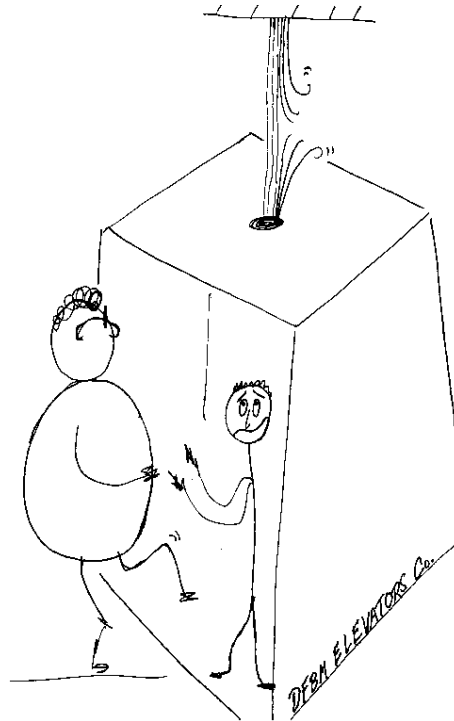


FIG. 1. The democratic fiber bundle model realized by an elevator rope.

The democratic fiber bundle model has further been applied to the study of cracks and fractures [7] and earthquakes [8], as a simplified model that retains some of the essential features of the original problem. In a failing medium, stress is continually redistributed due to the nucleation, growth, and coalescence of cracks. Realistic descriptions of fractures

and earthquakes may lie anywhere between this democratic or infinite-range limit embodied by the democratic fiber bundle model, also sometimes referred to as the “global-load-sharing” or “equal-load-sharing” model, and the local or short-range limit, the “local-load-sharing” model [9], in which the stress released by a broken bond is passed on to its immediate (intact) neighbors. Far from being one-dimensional or democratic, real-world systems may be (effectively) two- or three-dimensional, with connectivity properties that lead to a more complicated and richer picture. Alluding to the applicability of the model to the testing of a cloth sample rather than a hank, Daniels himself recognized [3] that “in closely woven fabrics the cross-threads afford a measure of support which introduces complications.”

Beyond the obvious question of the bundle’s strength (maximum sustainable stress without full rupture) addressed by Peirce [2] and Daniels [3], we would like to uncover, in the large  $N_0$  limit, its behavior characterized by the number  $N(F)$  of intact fibers as the force  $F$  increases from 0 to  $\infty$ . In particular, we investigate the critical properties of the fiber bundle upon approaching a macroscopic failure, and the generic classes in which they fall.

Upon incrementing the force from  $F - dF$  to  $F$ , a few fibers whose thresholds have been overshoot, break. As a result, the stress increases on the remaining intact fibers, leading to a secondary set of failures. This triggers a tertiary set of failures, and so on, until the bundle stabilizes at a non-vanishing  $N(F)$  or snaps off as a whole ( $N(F) = 0$ ). Consider the  $i$ th rupture which leaves  $N_i$  unbroken fibers, each now under a stress  $F/N_i$ . The thresholds of a fraction of intact fibers have been exceeded, namely  $\int_{F/N_{i-1}}^{F/N_i} p(x)dx$ , and the next set of failures brings their number down to

$$N_{i+1} = N_i - N_0 \int_{F/N_{i-1}}^{F/N_i} p(x)dx = N_0 \left\{ 1 - P \left( \frac{F}{N_i} \right) \right\}, \quad (1)$$

where  $P$  is the cumulative distribution defined by

$$P(x) = \int_0^x p(x')dx'. \quad (2)$$

Clearly, the function  $N(F)$ , defined as the number of fibers remaining unbroken under a total force  $F$ , is none other than  $N_\infty$  calculated at  $F$  (the limiting value of  $N_i$  as  $i \rightarrow \infty$ ).

Problems stated in terms of a recursion relation often have an elegant graphical solution which displays in a single picture the presence or absence of convergence. Here, a graphical scheme for the iteration is best constructed with the quantities  $x_i = N_i/F$ ,  $f = F/N_0$ , and

$$\pi(x) = 1 - P \left( \frac{1}{x} \right), \quad (3)$$

in terms of which Eq. (1) becomes

$$fx_{i+1} = \pi(x_i). \quad (4)$$

The function  $\pi(x)$  increases monotonically from 0 at  $x = 0$  to 1 at  $x = \infty$  and a graphical iteration of Eq. (4) shows that  $N(F) = N_\infty$  is given by the right-most intersection of the curve  $y = \pi(x)$  with the straight line  $y = fx$ . As the force is increased, the straight line becomes steeper and the abscissa  $N(F)/F$  of the intersection point moves to the left. Figure 2 illustrates the graphical scheme for three successive increments of the force. First,  $f$  is switched from 0 to  $f_1$ ; for  $f \rightarrow 0$ , the straight line is flat and intersects  $\pi(x)$  at  $x = \infty$  (as expected from  $x_0 = N_0/F$ ) and  $y = 1$ . After the sudden switch, fibers with a threshold smaller than  $f_1$  immediately break, causing more ruptures according to Eq. (4). The corresponding iterations are represented by dotted arrows, and terminate at the intersection point with abscissa  $x_\infty(f_1)$ . Next,  $f$  is switched from  $f_1$  to  $f_2$ , and similarly,  $x_i$  converges to  $x_\infty(f_2)$ . Finally,  $f$  is switched to  $f_3$ , and the iterations lead all the way to  $x = 0$ , which corresponds to a fully ruptured bundle. If the force, rather than suddenly switching from  $f_1$  to  $f_2$ , goes through several intermediary steps,  $x$  successively converges to the abscissa of the corresponding intersection points, but again ends up at  $x_\infty(f_2)$  when  $f = f_2$ . Thus  $N(F)$  is a well defined function of  $F$ , independent of the past history of the force as long as it is increased monotonically.

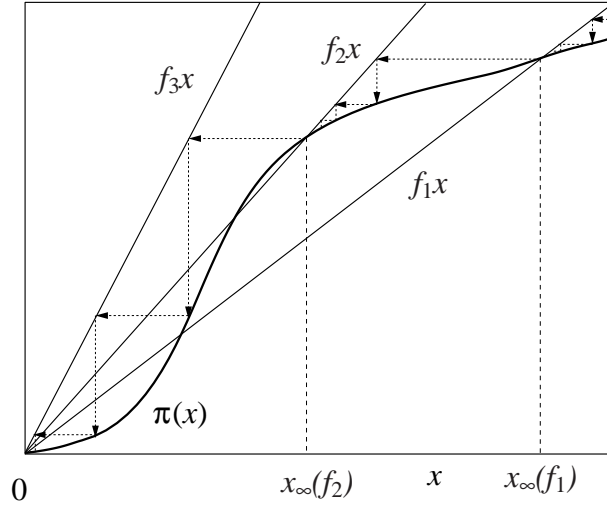
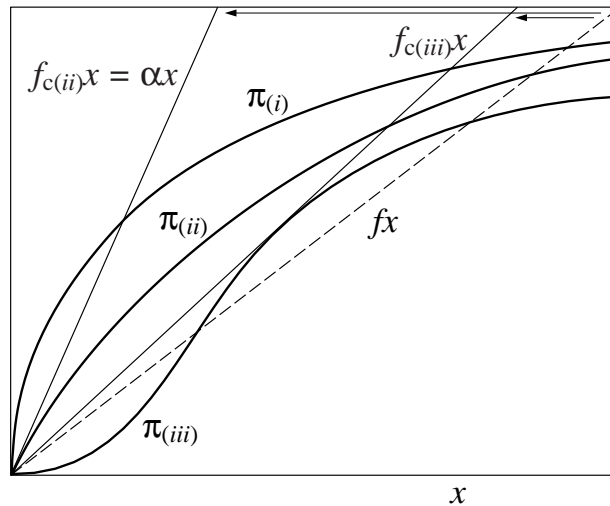


FIG. 2. Illustration of the graphical scheme for three successive increments in the force. The dotted arrows represent iterations of Eq. (4). The latter terminate, for each value of the force, at the right-most intersection, yielding the number of intact fibers as  $N(F) = Fx_\infty$ .

In what follows, we focus on a continuous steady increase of  $F$ , which can be thought of as the limit of many small successive increments. We assume that the iterations occur fast enough, or equivalently, that  $F$  varies slowly enough for the convergence to be considered immediate. By analogy to thermodynamical processes, we may say that the force is increased *quasi-statically*.

We are now in a position to investigate the critical behavior of the democratic fiber bundle model with various threshold distributions  $p(x)$ . The graphical method provides generic conclusions, based on a (drawn) arbitrary curve  $y = \pi(x)$ . Thus the results are independent of a specific analytical or numerical form for  $p(x)$ , but follow from the qualitative features of the curve. The latter identify a class of distributions, associated with a given behavior of the bundle. For continuous distributions, there are *three generic classes* [4], as illustrated in Fig. 3. These classes are distinguished by the character of  $p(x)$  at large argument, which dictates the bundle's behavior under large forces, through the slope

$$\frac{d\pi(x)}{dx} = \frac{1}{x^2} p\left(\frac{1}{x}\right). \quad (5)$$



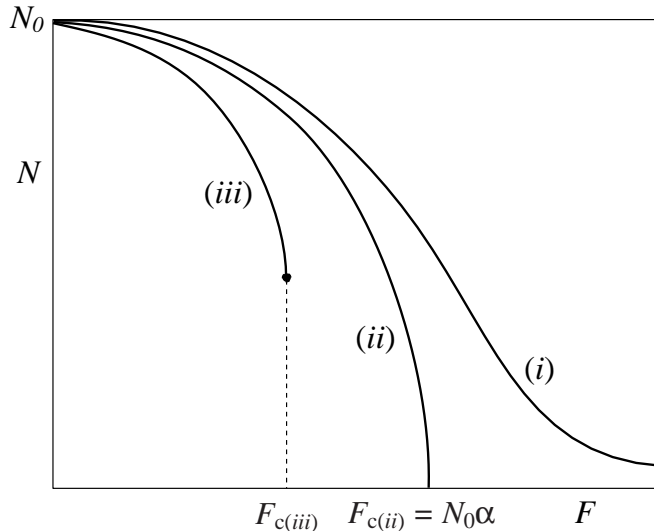


FIG. 3. The democratic fiber bundle model with continuous threshold distributions. (a) Illustration of the graphical scheme. As the force is increased, the straight line becomes steeper and the abscissa of the intersection points, proportional to the number of intact fibers, move to the left. Typical solutions are shown in (b). Intact fibers are always left in bundles of type (i), which never rupture completely. Bundles of type (ii) fail continuously at a force  $F_{c(ii)} = N_0\alpha$ , whereas bundles of type (iii) fail discontinuously at  $F_{c(iii)}$ .

*Class (i).* For  $p(x) \sim x^{-r}$  ( $x \rightarrow \infty$ ) with  $r < 2$  (normalization requires  $r > 1$ ), that is, distributions with an appreciable fraction of robust fibers, the bundle never fails completely. Under any force  $F$ , some intact fibers are left.

*Class (ii).* In the limiting case where  $p(x) = \alpha x^{-2}$  as  $x \rightarrow \infty$ , the number of intact fibers goes continuously to zero at  $F_c = N_0\alpha$ . Furthermore, the response function of the bundle or *breaking rate*  $dN/dF$  diverges as  $(F_c - F)^{-1/s}$ , where  $s$  is the subleading power entering the distribution function,  $p(x) = \alpha x^{-2} + \beta x^{-s} + \dots$ ,  $s > 2$ . Following the nomenclature adopted in the field of critical phenomena, we may refer to the macroscopic rupture of the bundle associated with a diverging response function as a second-order transition with exponent  $\gamma = 1/s$ .

An example of a “fat-tail distribution” is  $p(x) = (\alpha/x^r) e^{-\alpha/x^{r-1}}$  for any  $\alpha$ , with  $1 < r < 2$  in class (i) and  $r = 2$  (and exponent  $\gamma = (2r - 1)^{-1} = 1/3$ ) in class (ii).

*Class (iii).* For any narrower distribution, such that  $x^2 p(x) \rightarrow 0$  for  $x \rightarrow \infty$ , there is a macroscopic failure of the bundle at a finite critical force  $F_c$  at which the number of intact fibers falls discontinuously from  $N(F_c)$  to 0. The breaking rate diverges in general as

$$\frac{dN}{dF} \sim (F_c - F)^\gamma, \quad \gamma = -\frac{1}{2}. \quad (6)$$

A “trivial” exponent of  $\gamma = -1/2$  is to be expected within a mean-field approach which ignores the effect of spatial fluctuations (see Sec. V). Of course, it is possible to choose a particular distribution with a “bump” such that  $\gamma = 1/2n$ , with  $n$  an integer, instead of  $\gamma = 1/2$ , but it reflects a fine-tuned choice rather than the generic one. All continuous distributions with finite mean, subsumed in class (iii), lead to a macroscopic failure of the bundle at a finite critical force, signaled by a diverging breaking rate. Although this divergence in the response is still reminiscent of a second-order transition, the situation differs from the usual case where the order parameter (here  $N(F)$ ) is continuous at the singularity. To avoid any confusion, we refer to ruptures of type (iii) as *soft failures*.

Two examples of distributions which belong to class (iii) are  $p(x) = (x/\lambda^2) e^{-x/\lambda}$  and  $p(x) = (x/\lambda) e^{-x^2/2\lambda}$ . Other examples include finite-support distributions, which are non-vanishing only in an interval  $\mathcal{I} = [x_0, x_0 + \lambda]$ , provided  $p(x)$  is continuous on  $\mathcal{I}$  and  $p(x_0) = p(x_0 + \lambda) = 0$ .

Fig. 3(b) illustrates the generic histories  $N(F)$  for each of the three classes. Clearly, by having more “bumps” ( $\pi^{(iii)}(x)$  on Fig. 3(a) has one), that is, variations in the convexity of  $\pi(x)$ , the bundle may undergo additional macroscopic (finite fraction of  $N_0$ ) failures at smaller forces. None of these, however, may lead to a complete rupture, which always corresponds to one of the three classes described above.

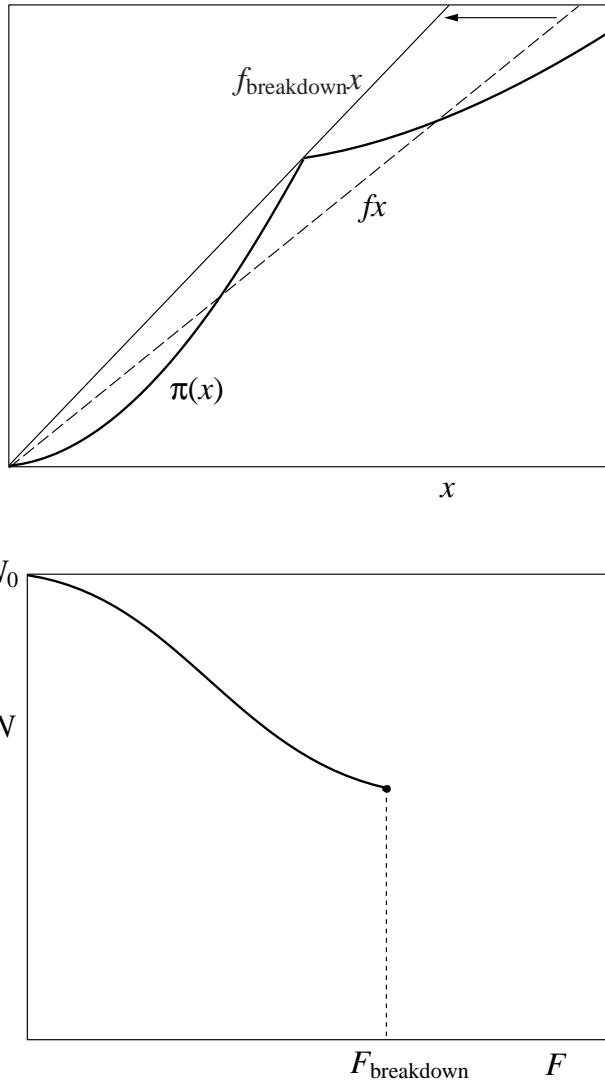


FIG. 4. The democratic fiber bundle model for a markedly discontinuous distribution of the thresholds. In (a), the graphical scheme leads to (b), an abrupt failure of the bundle.

The examples given for class (iii) are valid for any value of the parameter  $\lambda$ . Thus, the threshold distribution may be as narrow and peaked ( $\lambda \rightarrow 0$ ) as desired and still lead to a soft failure, provided  $p(x)$  is continuous. An *abrupt* rupture of the bundle *with no divergence in the breaking rate* preceding it is possible only if  $\pi(x)$  has a non-differentiable point (Fig. 4) [4], which in turn requires a discontinuity in  $p$ . Thus, abrupt failures in this mean-field model, far from being a generic feature associated with narrow disorder distributions, are an artifact of a singular point in  $p$ . The phenomenon is in fact even more particular, because the *magnitude* of the discontinuity matters. In the case of a finite-support distribution on  $\mathcal{I}$  with  $p(x_0) \neq 0$ , for example, no fiber breaks up to a force  $F_0 = N_0 x_0$ . At  $F_0$ , an abrupt failure occurs only if  $d\pi(1/x_0)/dx \geq x_0$ , as can be shown by the graphical method, which requires a minimal jump  $p(x_0) \geq 1/x_0$ . Whether this macroscopic failure yields full rupture of the bundle or not depends on the detailed form of  $p$ . If it does not, and if  $p$  is continuous on  $\mathcal{I}$ , the global bundle failure is soft and belongs to one of the three cases examined above (case (iii) if  $\langle x \rangle = \int_0^\infty dx x p(x) < \infty$ ). The description of a large  $N_0$  bundle by a continuous distribution  $p$  would seem more physical, unless it is made of fibers of a few different types, each with a well defined threshold. Consider for example a “bimodal” bundle with  $\rho N_0$  ( $0 \leq \rho \leq 1$ ) fibers of strength  $f_1$  and  $(1 - \rho) N_0$  fibers of strength  $f_2 < f_1$  [3]. It is easy to see from the graphical method (Fig. 5) that if  $f_2/f_1 > \rho$ , the entire bundle snaps off abruptly at  $F_2 = N_0 f_2$ . On the other hand, if  $f_2/f_1 < \rho$  it undergoes an abrupt failure at  $F_2$  leaving the  $\rho N_0$  stronger fibers intact, and then ruptures completely (again abruptly) when the force reaches  $F_1 = N_0 f_1$ .

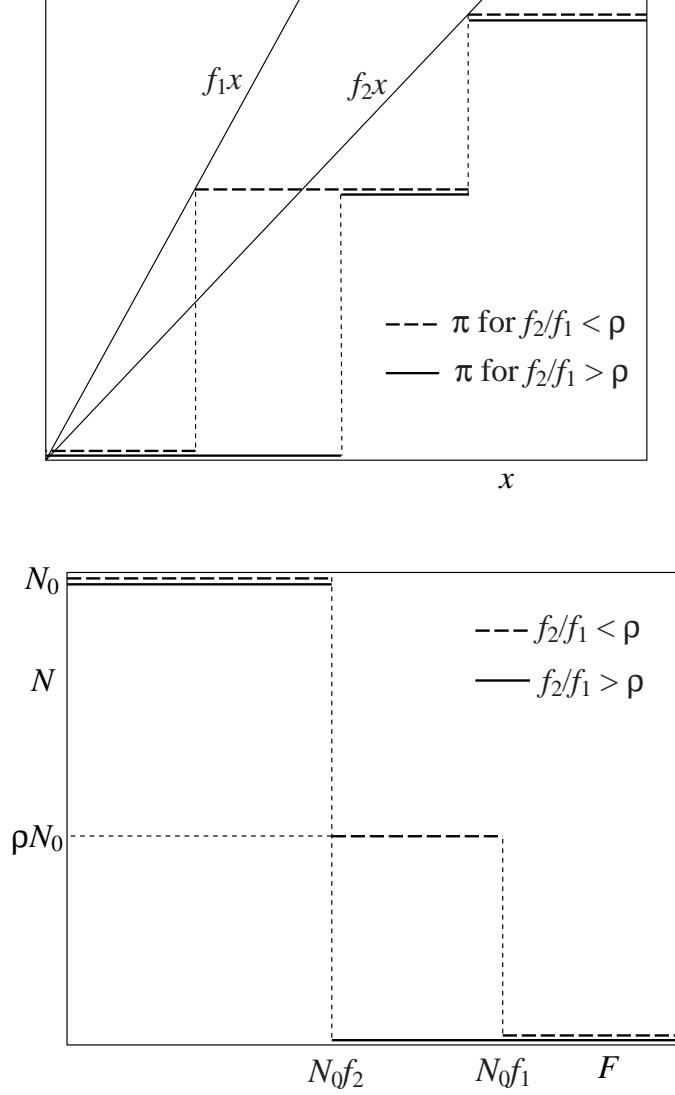


FIG. 5. The democratic fiber bundle model for a “bimodal” distribution consisting in  $\rho N_0$  fibers of strength  $f_1$  and  $(1 - \rho) N_0$  fibers of strength  $f_2$ . (a) Illustration of the graphical scheme and (b) typical solutions. The bundle fails in either one or two abrupt steps.

A physical medium which fails as a result of the growth of a single large crack is often referred to as “ductile,” in analogy with flexible materials, such as most metals, which rearrange under stress and can thus be pulled into long thin threads. At the other end of the spectrum, fragile or “brittle” media are characterized by a sudden failure due to the coalescence of many microcracks. In the context of our mean-field model, we may identify abrupt failures from markedly discontinuous distributions (such as narrow finite-support ones or bimodal ones) with brittleness, and soft failures from the continuous distributions of classes (ii) and (iii) with ductility. Thus the character of a medium’s strength depends on the *shape* of the distribution of randomness.

The failure of an element, whether a fiber in an elevator rope or a patch of a tectonic plate, is often accompanied by the emission of a sound [10]. Before an abrupt failure, nothing unusual is heard, whereas an increasingly loud noise is produced by a soft failure. Thus impurities, dirt, and disorder might be salutary in times of calamity!

### III. SOCIAL LOGISTICS: THE BOARDING GATE PROBLEM

Armed with the method developed in Sec II, we return to the boarding-gate problem of the introduction, and treat it in a quantitative fashion. The similarity between the breaking of a fiber bundle and the growth of a boarding-gate line becomes more apparent through the following mapping of the degrees of freedom, disorder, driving agent, and coupling:

sitting person, waiting	$\longleftrightarrow$	intact fiber,
standing person, in line	$\longleftrightarrow$	broken fiber,
“obedience threshold”	$\longleftrightarrow$	strength threshold,
flight attendant’s calls	$\longleftrightarrow$	driving force,
temptation from seeing the line	$\longleftrightarrow$	redistribution of the force.

Nevertheless, the two problems are different in that the stress applied to any one intact fiber is inversely proportional to their total number, whereas the temptation here grows with the length of the line. Furthermore, for simplicity we focus on a single call of the flight attendant, say the first one. In the language of the democratic fiber bundle model, this corresponds to switching the force from zero to some value, and leaving it there. Finally, the “thermodynamic limit” we treat (in implicitly assuming infinitely many passengers) may be a poor approximation for a situation involving a few dozen or a few hundred people. The fact that the first group of passengers called, and consequently the ones still waiting, may not be representative of the overall threshold distribution, for example, is one of the possibly important finite-size effects neglected.

Let us say that the flight attendant first calls  $\ell$  passengers, who readily form a line. Seeing the latter, a few disobedients join in, equal in number to  $(N - \ell)P(\ell)$ , where  $N$  is the total number of passengers waiting to board the flight and  $P$  is the cumulative threshold distribution. More precisely,  $p(x)dx = (dP/dx)dx$  is the probability that an individual unduly joins the line, when it reaches a length between  $x$  and  $x + dx$ . The process might stop at this point, leaving the few intruders in line, or might keep on “avalanching.” In general, we can write a recursive relation describing the growth of the line, analogous to Eq. (1), as

$$n_{i+1} = \ell + (N - \ell)P(n_i), \quad (7)$$

where  $n_i$  is the number of people in line after  $i$  iterations ( $n_0 \equiv \ell$ ). The avalanching terminates at the left-most intersection of the line  $(n - \ell)/(N - \ell)$  with the curve  $P(n)$  and the eventual length of the line,  $n_\infty$ , is read off as the abscissa of the intersection point. In other words, the length of the line is obtained as the smallest solution to

$$\frac{n - \ell}{N - \ell} = P(n), \quad (8)$$

leading to the following possible scenarios.

- Most optimistically, no one’s threshold is lower than the length of the initial line, that is,  $p(x \leq \ell) = 0$  (Fig. 6). No unexpected passenger shows up in the line, and the boarding runs smoothly.
- More generally, for a large airplane with hundreds of passengers, we expect thresholds to be widely distributed. We consider distributions with  $p(x) \neq 0$  for all  $x \in [0, N]$  and  $P(N) = 1$ , according to which there are always some disobedients who join the ranks no matter how small the temptation and no one is restrained enough to stay seated when the line includes nearly all the passengers. In this case, the behavior of the line’s growth is governed by the character of  $p$  at large argument (Fig. 7), reminiscent of the solution of the democratic fiber bundle model with continuous distributions. If  $p(N) < 1/N$ , the line may anarchically absorb all passengers. If  $p(N) > 1/N$ , on the other hand, it must stabilize at  $\ell < n_\infty < N$ , the precise value of which depends on the detailed form of the function  $p$ .



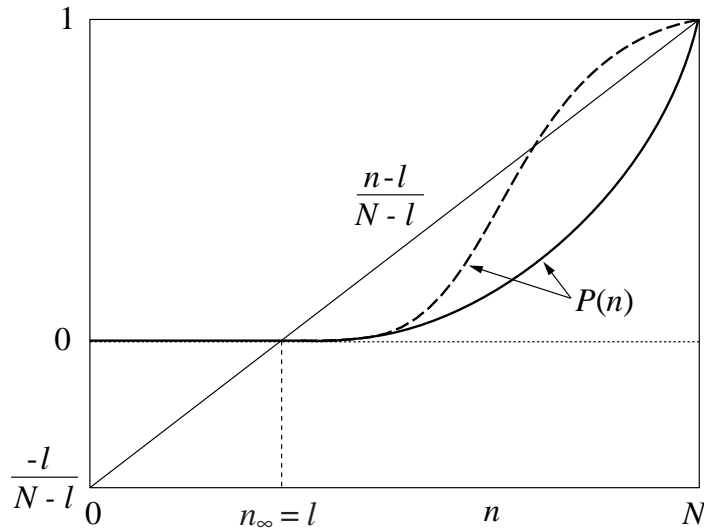


FIG. 6. Graphical scheme for the boarding-gate problem with a threshold distribution vanishing below  $\ell$ . The solid and dashed curves represent two possible cases, both leading to lines with no intruders.

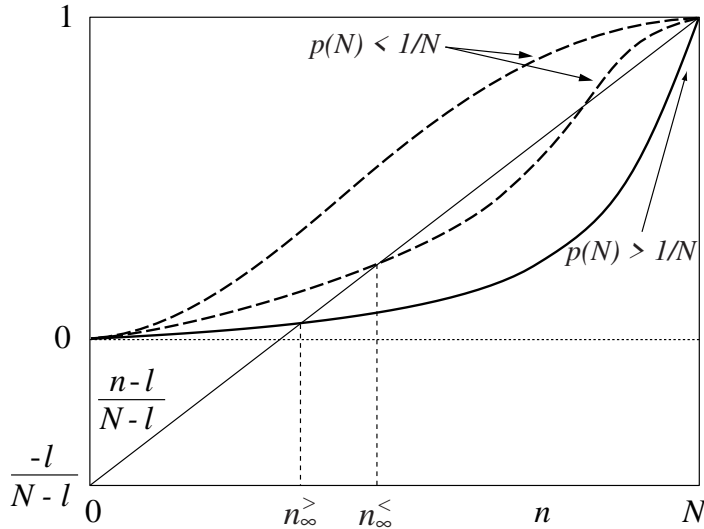


FIG. 7. Graphical scheme for the boarding-gate problem with non-vanishing distributions. If  $p(N) > 1/N$  (solid line),  $P(n)$  must cross the straight line  $(n - \ell) / (N - \ell)$  at some  $n$  smaller than  $N$ . If  $p(N) < 1/N$  (dashed lines), it may or may not.

- Often, there is a small fraction  $n_p/N$  of *complete* disobediends, a small fraction  $n_s/N$  of *complete* obediends, and the rest of the passengers' thresholds scattered in between. For such a contingency, the distribution reads

$$p(x) = \frac{n_p}{N} \delta(x) + g(x) + \frac{n_s}{N} \delta(x - N), \quad (9)$$

where  $g(x)$  is a smooth function which, in a realistic model, is appreciable between two bounds  $n_1$  and  $n_2$ . Then, the growth of the line saturates at a length  $\ell + (\frac{N-\ell}{N}) n_p < n_\infty < N - (\frac{N-\ell}{N}) n_s$ , which depends on the relative values of  $\ell$ ,  $n_p$ , and  $n_1$  (Fig. 8). If  $n_1 > \ell + n_p$ , the eventual line includes few unexpected passengers except the physicists — a situation easy to cope with, due to the small number of physicists. However, if  $n_1 < \ell + n_p$  (and in particular if  $n_2 - n_1$  is small ( $g$  very peaked)), the few physicists drag flocks of others along, resulting in a line with all the passengers but the complete obediends and perhaps a few highly obedient individuals.

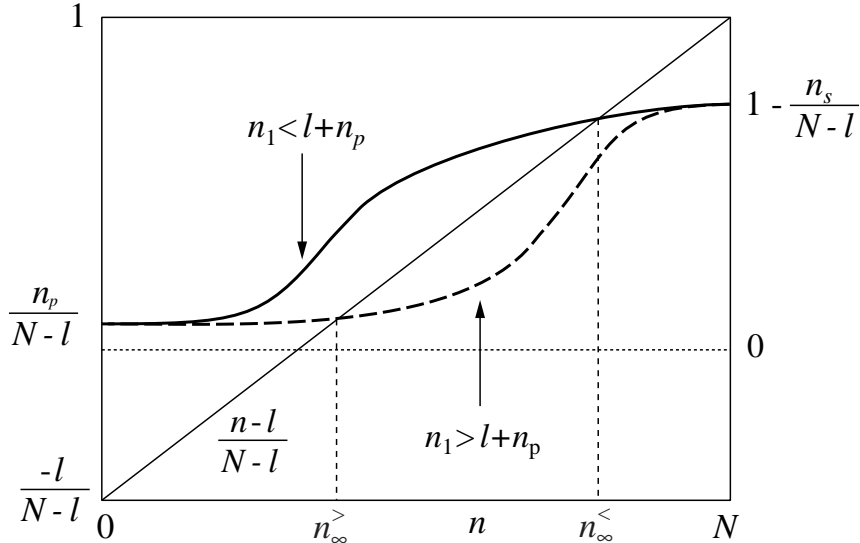


FIG. 8. Graphical scheme for the boarding-gate problem with a distribution reflecting a fraction of complete disobedients, a fraction of complete obedient, and the rest of the passengers peaked in between. The character of the solution depends on whether the peak is closer to the disobedient (solid line) or to the obedient (dashed line) side.

There is no doubt that social phenomena involve a great many parameters making them highly complex in comparison to “simple” physical systems such as a fiber bundle. However, in much the same way as the breaking of a wool hank is faithfully described without recourse to the molecular structure of the individual threads, a *coarse* picture of some human phenomena may be drawn while ignoring intricate psychological and other processes that each individual goes through. And it is amusing that such a *phenomenological* approach yields a number of quantitative, testable results for the behavior of a human group.

#### IV. MAGNETS OUT OF EQUILIBRIUM: CRITICAL HYSTERESIS IN A DRIVEN ISING MODEL

In the most modest speck of dust, an incredible number of electrons are dancing around, creating small currents and with them magnetic moments. Each electron also carries its own spontaneous moment, and it is the complicated addition of all these effects which determines the total magnetization of the dust. In the spirit of foregoing intricate details in favor of a coarser but simpler picture, Ising and Lenz proposed a model [11] in which a material is divided into many elements (labeled by their position  $\mathbf{r}$ ), each carrying a (unit) magnetic moment, or *spin*, which tends to align with the local magnetic field it experiences, like a little compass. In the so-called “Ising model,” the spins are constrained to a given direction, may point upward ( $m(\mathbf{r}) = +1$ ) or downward ( $m(\mathbf{r}) = -1$ ). The average magnetization is defined as

$$M = \frac{1}{N} \sum_{\mathbf{r}} m(\mathbf{r}), \quad (10)$$

where  $N \rightarrow \infty$  is the total number of spins, and the local field is composed of the applied field and the one created by neighboring spins. On a mean-field level, one assumes that the system may still be faithfully described if the many degrees of freedom are reduced to a single quantity, here the average magnetization. This assumption becomes exact if the interaction between spins is infinite in range, that is, all spins interact with all others in the same way, so that they contribute to the local field equally everywhere. Even if the coupling has a limited range, we can imagine that such an approach becomes more and more accurate as the dimensionality is increased, as spins acquire more and more neighbors, thus “averaging out” their contributions to the local field. In fact, the mean-field approximation yields the correct critical behavior above a given, *finite* dimension (see Sec. V).

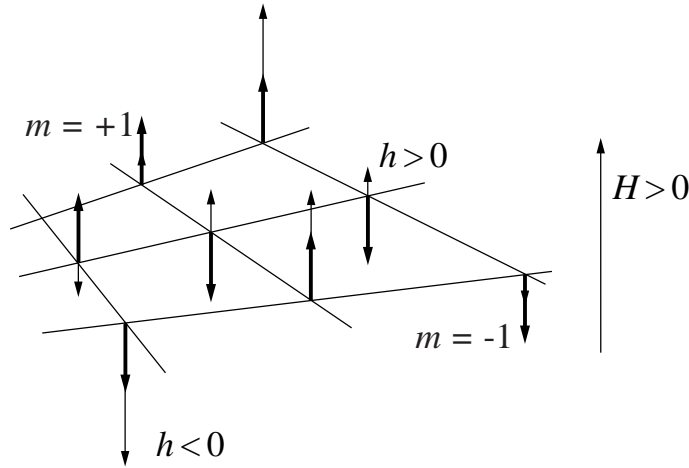


FIG. 9. Illustration of a few “sites” of a two-dimensional Ising model with a random field. The thick arrows represent the spins which can point upward ( $m = +1$ ) or downward ( $m = -1$ ), and the thin arrows represent the random field  $h$ . Each spin experiences a uniform applied field  $H$ .

We confine our study to zero temperature, so that spins are always perfectly aligned with the local field, forbidding any *thermal* fluctuation. In real materials, however, the presence of impurities leads to *random* fluctuations. In many cases, the effect of the impurities is to perturb the local magnetic field which acquires a stochastic component in addition to a uniform one (Fig. 9) [14]. More precisely, the mean-field, driven, disordered version of the Ising model, first introduced in Ref. 6, is defined by a local field

$$f(\mathbf{r}) = H + h(\mathbf{r}) + JM, \quad (11)$$

where  $H$  is a uniform field (chosen by the experimentalist),  $h$  is a *random field* chosen at each position  $\mathbf{r}$  from some probability distribution  $p(h)$ , and  $J > 0$  represents the strength of the spin-spin coupling. The configuration of the system is then given by the “alignment rule”

$$\begin{cases} m(\mathbf{r}) = -1 & \text{if } f(\mathbf{r}) < 0 \Leftrightarrow h(\mathbf{r}) < -H - JM, \\ m(\mathbf{r}) = +1 & \text{if } f(\mathbf{r}) > 0 \Leftrightarrow h(\mathbf{r}) > -H - JM. \end{cases} \quad (12)$$

How does the driven disordered Ising model evolve when the (driving) field  $H$  goes from  $-\infty$  to  $\infty$ ? Initially ( $H = -\infty$ ), all the spins point downward ( $m = -1$ ). As  $H$  is increased from  $-\infty$ , the local fields with large positive random fields soon become positive, and the associated spins flip upward. These flips further increases the local field, which induces new spin flips, and so on. Once  $H$  is incremented enough, the negative  $h$ 's tend to pin the corresponding spins downward, and the configuration results from the competition between the driving agent  $H$ , the “restoring” force  $JM$ , and the pinning forces  $h$  — a common scenario for forced or driven random media [15,16].

The avalanching present in this simple model is reminiscent of fracture phenomena [5], and the driven disordered Ising model can be mapped to the democratic fiber bundle model as

downward spin ( $m = -1$ )	$\longleftrightarrow$	intact fiber,
upward spin ( $m = +1$ )	$\longleftrightarrow$	broken fiber,
random field ( $h$ )	$\longleftrightarrow$	strength threshold,
uniform field ( $H$ )	$\longleftrightarrow$	driving force,
spin-spin coupling ( $J$ )	$\longleftrightarrow$	redistribution of the force.

As in the case of the boarding gate problem, the main difference with the democratic fiber bundle model arises from the way in which the individual degrees of freedom interact, and the iterative equation for the fraction  $n_\downarrow$  of downward spins, in the driven disordered Ising model, reads

$$n_{\downarrow i+1} = P(-H - JM_i), \quad (13)$$

where  $P(x) = \int_{-\infty}^x p(h)dh$  is the cumulative distribution function. Equivalently, in terms of the magnetization  $M = 1 - 2n_\downarrow$ ,

$$M_{i+1} = 1 - 2P(-H - JM_i). \quad (14)$$

As before, the right-hand-side is a monotonically increasing function of the avalanching variable  $M_i$ , and the so-called *hysteresis* curve  $M = M_\infty(H)$  is given by the left-most intersection of  $y(M) \equiv 1 - 2P(-H - JM)$  with the bisector ( $y = x$ ).

Rather than considering all possible types of disorders, we focus on three, commonly encountered in the literature [17,18].

(1) *Gaussian disorder*:  $p(h(\mathbf{r})) = \frac{1}{\sqrt{2\pi\sigma^2}} e^{-h^2/2\sigma^2}$ . As  $H$  is increased, the curve  $y(M)$  is translated to the left and the intersection point consequently moves up (and to the right). Three qualitatively different solutions are obtained, depending on whether the maximum slope  $y'(M = -H/J) = 2J/\sqrt{2\pi\sigma^2}$  is greater, equal, or lesser than 1 (Fig. 10).

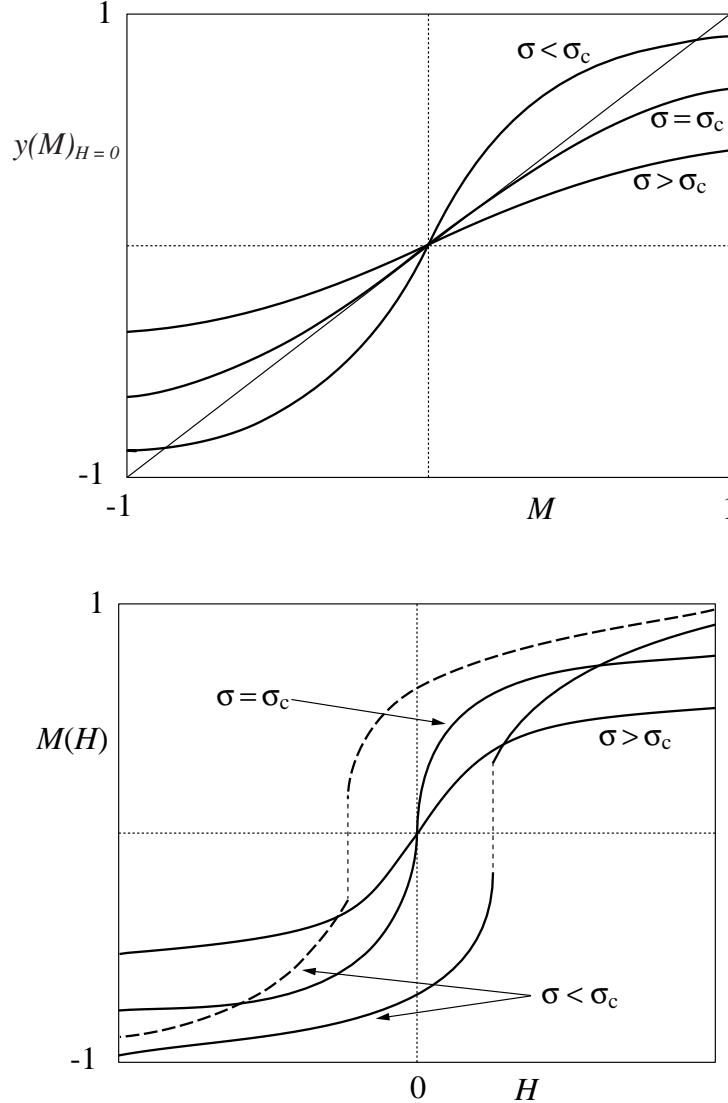


FIG. 10. The driven Ising model with a Gaussian random field. (a) Illustration of the graphical scheme for sub-critical, critical, and super-critical values of the disorder. The curves  $y(M)$  are drawn at  $H = 0$ ; as  $H$  is increased, they move to the left, starting in the far right at large negative  $H$  and ending in the far left at large positive  $H$ . (b) Corresponding typical magnetization, or hysteresis, curves. The dashed line represents the case of a decreasing  $H$ , in the sub-critical regime. In the critical and super-critical regimes, the curves for increasing and decreasing  $H$  are superposed.

- $\sigma < \sigma_c \equiv \sqrt{2/\pi}J$ : For a small disorder, there is a jump in the magnetization at some field  $H_{\text{jump}} > 0$ ), signaled, as in the democratic fiber bundle model, by a square root divergence of the response function or susceptibility

$$\chi = \frac{dM_\infty}{dH} \sim (H_{\text{jump}} - H)^{-1/2}. \quad (15)$$

Larger values of  $\sigma$  reduce the magnitude of the discontinuity, which ultimately shrinks to a point at  $\sigma = \sqrt{2/\pi}J$ .

- $\sigma = \sigma_c$ : A specific value  $\sigma_c$  of the disorder yields a *critical* hysteresis curve, which, although continuous, displays a singular point at  $H = M = 0$ . Expanding  $y(M)$ , we easily obtain the nature of the singularity, as

$$\chi(H \rightarrow 0) \sim H^{-2/3}. \quad (16)$$

In a more general line of reasoning (see Sec. V), we note that the asymmetry of  $y$  about the origin (at  $H = 0$ ) rules out even powers relating  $M$  to  $H$  as

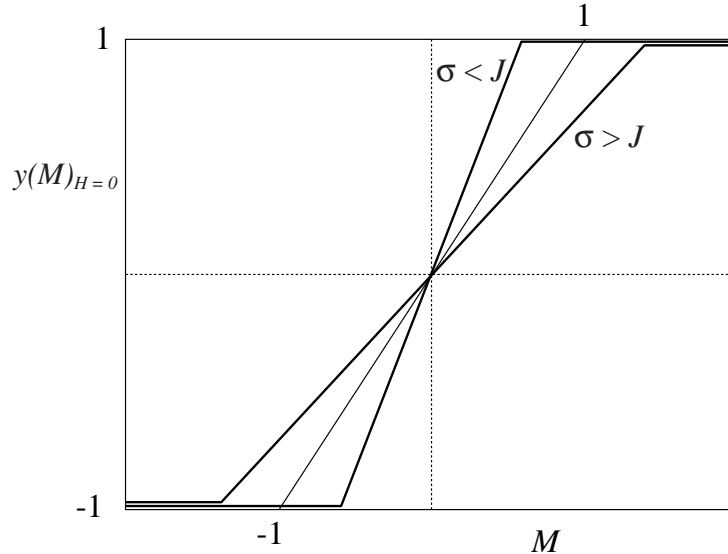
$$H \sim M^{2n} + \text{higher powers}, \quad (17)$$

and in particular a quadratic dependence  $H \sim M^2$ , leaving a cubic behavior  $H \sim M^3$  as the best candidate; inverting and differentiating readily leads to Eq. (16).

- $\sigma > \sigma_c$ : At large disorders, the magnetization curve is smooth, with a finite susceptibility everywhere.

Figure 10(b) shows generic curves corresponding to the above three cases. This phase diagram is very similar to that of the democratic fiber bundle model (classes (i)–(iii)), in that a discontinuous, first-order-like region terminates at a critical, or second-order, point with a different (non-trivial) exponent. In fact, it is believed [19,20] that, while the global phase diagram is unchanged in a local theory extending beyond a mean-field approach, the precursor divergence of Eq. (15) is suppressed, resulting in proper first-order behavior. (If a similar conclusion applies to fracture phenomena, it might help to explain the presumably abrupt failures often observed.) Furthermore, as  $\sigma$  approaches  $\sigma_c$  from below,  $H_{\text{jump}}$  decreases to zero, progressively hampering the hysteretic (lagging) nature of the solution; for  $\sigma \geq \sigma_c$ , both the remnant and coercive fields are vanishing. Again, this is an artifact [20] of the present formulation. These remarks point at the tip of an iceberg onto which the mean-field approximation often runs.

(2) *Uniform disorder*:  $p(h(\mathbf{r})) = 1/2\sigma$  for  $-\sigma \leq h \leq \sigma$  and vanishes elsewhere. This form may be viewed as a “digitized,” roughened, or sharpened version of Gaussian disorder. Again, the character of the solution depends on the magnitude of the slope  $y'(M = -H/J) = J/\sigma$  relative to 1 (Fig. 11).



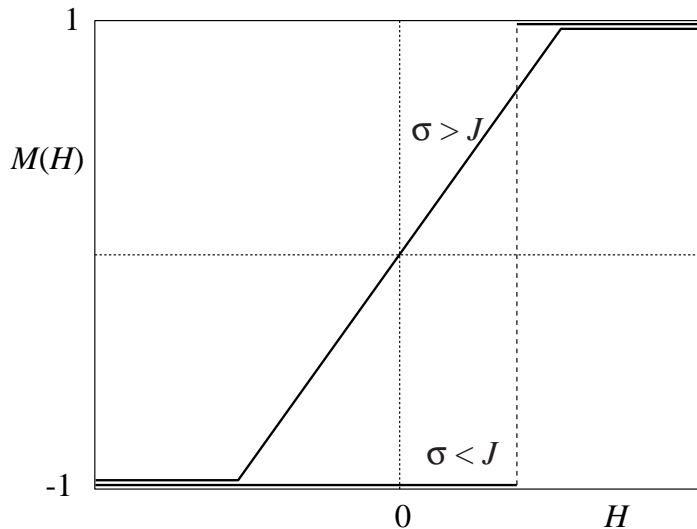
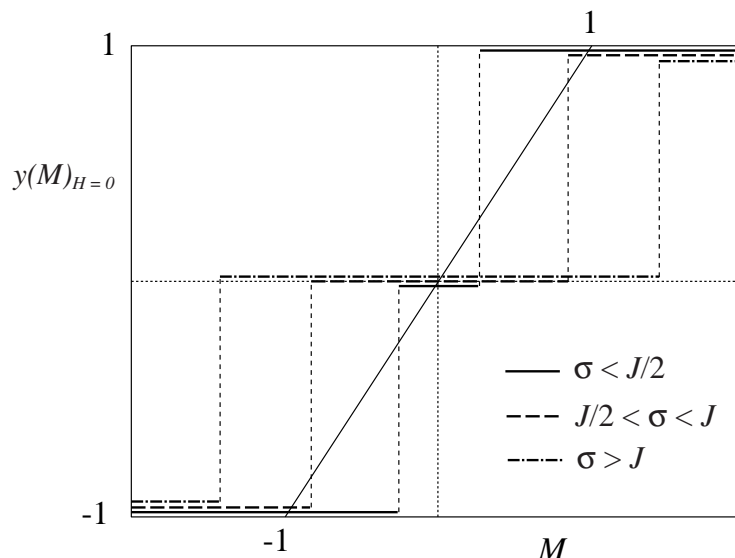


FIG. 11. The driven Ising model with a uniform random field. (a) Illustration of the graphical scheme and (b) typical solutions.

- If  $\sigma < J$  (small disorder), the magnetization switches from  $-1$  to  $+1$  at  $H_{\text{jump}} = J - \sigma > 0$ .
- If  $\sigma > J$  (large disorder), the magnetization is continuous and piecewise linear; it starts to increase linearly from  $-1$  at  $H = J - \sigma$ , and reaches  $+1$  at  $H = \sigma - J$ .

As in the previous examples, the nature of the solution varies significantly from one type of disorder to the next. In particular, we note that the discontinuity of the uniform distribution rules out any divergence or critical point, in agreement with our observations for the democratic fiber bundle model.

(3) *Bimodal disorder*:  $p(h(\mathbf{r})) = [\delta(h + \sigma) + \delta(h - \sigma)]/2$ . The bimodal distribution is often used as an alternative to the Gaussian distribution, notably in computer simulations. It represents an even more “digitized,” or sharpened, version of disorder, reminiscent of the democratic fiber bundle model with fibers of two different types. The graphical scheme is illustrated in Fig. 12, along with typical solutions which fall, as above, into one of two classes. The phase diagram is especially simple to understand for a bimodal disorder, which limits random fluctuations as much as possible and reduces the problem to a two-body one. Half of the spins (those with  $h = +\sigma$ ) flip upward when  $H$  reaches  $H_{\text{jump}1} = J - \sigma$ , leading to a vanishing magnetization. This further triggers the flipping of the remaining spins if their (updated) local field  $f = H_{\text{jump}1} - \sigma$  is positive, that is, if  $\sigma < J/2$  (small disorder), resulting in a global switch from  $M = -1$  to  $M = +1$  at  $H_{\text{jump}1}$ . If  $\sigma > J/2$  (large disorder), on the other hand, the magnetization remains at zero until the local field changes sign, at  $H_{\text{jump}2} = \sigma$ , when the remaining downward spins flip to yield  $M = +1$ .



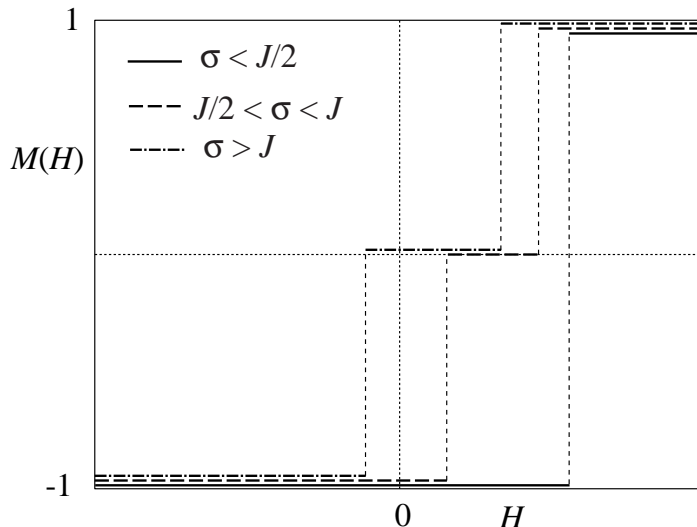


FIG. 12. The driven Ising model with a bimodal random field. (a) Illustration of the graphical scheme and (b) typical solutions.

In contrast to the Gaussian and uniform cases, the large-disorder phase *exhibits hysteresis*:  $M(H)$  is not symmetric about  $H = 0$ , there is a remnant magnetization  $M = -1$  (if  $H_{\text{jump}1} > 0$  that is,  $\sigma < J$ ) and a coercive field which can be defined as  $H_{\text{jump}2}$ . Clearly, a hysteretic behavior originates in the coexistence of more than one possible solution to a dynamical system [21]. Rather than being chosen by an optimum principle, the actual, physical solution follows from the *history*, or, in the case of a monotonically increasing  $H$ , from the *initial conditions*. Thus, *metastability* and hysteresis are intimately related. The random fluctuations tend to pin the system to a metastable state. The thermal fluctuations, which we have ignored, play an opposite part in sweeping the system in its configuration space, thus favoring ergodicity. An important question relates to the interplay of these two effects. It is believed that disorder generally dominates and that thermal fluctuations are irrelevant at criticality, both in equilibrium [14] and in non-equilibrium [6,19–21] problems.

## V. DIGRESSION: EFFECTIVE THEORIES

The path from elementary laws to the multitude of fascinating observed phenomena is definitely not a straight and plain one. The situation is a bit like that of a shadow show in which shadows of dragons, wolves, and birds, are cast on a white drape by the moving hands of a pantomime. The goal is to understand the unfolding story. Focusing on the artist’s hands is probably not the most fruitful tactic, and surely not the easiest. The shadows allow a more direct grasp of the story by retaining the important aspects of the hands’ intricate movements and shapes, while smearing away irrelevant details such as the nails or the hair on the fingers. In theoretical physics, the mime’s hands are the fundamental laws, and the shadows are *effective* or *phenomenological* theories.

Hydrodynamics constitutes a prominent example of an effective theory, where the molecular nature of a fluid is disregarded in favor of a description in terms of a homogeneous medium. The collective motion of hundreds or millions of particles is reduced to that of their center of mass, that is, to a local average, which smears out a large number of details and fine characteristics, leaving a framework with a smaller number of variables than the original one. Typically, a fluid is then described by fields of density, velocity vector, and temperature — five quantities associated with each point in space and time substitute for the many molecular degrees of freedom around that point.

A delicate question relates to how much of the finer print, or *fluctuations*, needs to be included for an accurate description of a given phenomenon at a given length scale. Various effective theories may be constructed to describe a given system, the ones with the fewest allowed fluctuations being termed “mean-field.” Often, spatial fluctuations are ignored altogether resulting in highly coherent behavior, and the system reduces to a single (or a few) degrees of freedom.

The hydrodynamic equations can be derived from symmetry and conservation principles alone. These principles are satisfied at the molecular level and unspoiled by any averaging procedure. Thus, an effective theory ensues from robust properties that span many length scales, and is free from a specific (mechanistic) model. It has lost the details

involved in the latter, but gained the sturdiness of generality: an effective formulation encompasses all possible models lying within the constraints imposed by a set of symmetries.

It is therefore worthwhile to construct a phenomenological theory of breakdown phenomena; in what follows, we shall concentrate on the driven disordered Ising model [6,20]. In addition to its robustness, an effective field theory offers an analytical framework in which the range of the coupling between spins, the dimensionality of the systems, or other aspects may be modified and studied in a unified fashion, and for which a number of powerful tools have been developed [22].

In the spirit of hydrodynamics, we consider a spin *field* or *density*  $s(\mathbf{r})$  regarded as a local average of magnetic moments at  $\mathbf{r} \in \mathfrak{R}^d$ , where  $d$  is the dimension of the system. Its value lies anywhere within an interval centered at zero, and we further generalize the problem by allowing  $s(\mathbf{r}) \in (-\infty, \infty)$ . Inspired by the model [6,20] of Sec. IV and its solution as given by  $y(M) - M = 0$ , we posit that the spin density at each point is obtained from an algebraic equation

$$f_{\mathbf{r}}(\{s(\mathbf{r})\}, H, h(\mathbf{r})) = 0 \quad (\text{for all } \mathbf{r}), \quad (18)$$

where  $H$  is a uniform applied magnetic field and  $h(\mathbf{r})$  is a Gaussian random field felt by the spins at  $\mathbf{r}$ . This system of equations may have more than one solution; if  $H$  is monotonically increased as before, the spins start off very negative, and the physical solution corresponds to the “left-most” one, with smallest (most negative)  $s(\mathbf{r})$ 's. If, rather,  $H$  is monotonically decreased from a high positive value, we expect the same set of solutions with an opposite sign, consistent with the *reflection symmetry*

$$f_{\mathbf{r}}(\{-s(\mathbf{r})\}, -H, -h(\mathbf{r})) = f_{\mathbf{r}}(\{s(\mathbf{r})\}, H, h(\mathbf{r})), \quad (19)$$

a first constraint on the form of  $f_{\mathbf{r}}$ . As before, the quantities of interest are the overall spatial average  $\langle s \rangle$  of  $s(\mathbf{r})$  and its response to the applied field. An effective, coarse-grained theory is clearly best suited to answer questions on the system's global properties, and in particular on its critical behavior which involves a collective response to an infinitesimal change in  $H$ . From the study of the driven disordered Ising model, we expect the critical point to occur at  $H = \langle s \rangle = 0$ . (We note that this is also a special point in terms of the symmetries, due to the *statistical invariance* under  $h \rightarrow -h$ .) Close to the latter, we may describe  $f_{\mathbf{r}}$  by an expansion in its arguments. In contrast to fluid dynamics or pure critical phenomena, here quenched disorder imposes some spatial fluctuations, which we limit by considering a small random field, leading to

$$\begin{aligned} f_{\mathbf{r}} = & \int d^d r' J(\mathbf{r}, \mathbf{r}') s(\mathbf{r}') + AH + Bh(\mathbf{r}) \\ & + \int d^d r' d^d r'' d^d r''' K(\mathbf{r}, \mathbf{r}', \mathbf{r}'', \mathbf{r}''') s(\mathbf{r}') s(\mathbf{r}'') s(\mathbf{r}''') \\ & + H \int d^d r' d^d r'' L(\mathbf{r}, \mathbf{r}', \mathbf{r}'') s(\mathbf{r}') s(\mathbf{r}'') + h(\mathbf{r}) \int d^d r' d^d r'' M(\mathbf{r}, \mathbf{r}', \mathbf{r}'') s(\mathbf{r}') s(\mathbf{r}'') \\ & + H^2 \int d^d r' N(\mathbf{r}, \mathbf{r}') s(\mathbf{r}') + h(\mathbf{r})^2 \int d^d r' O(\mathbf{r}, \mathbf{r}') s(\mathbf{r}') + Hh(\mathbf{r}) \int d^d r' P(\mathbf{r}, \mathbf{r}') s(\mathbf{r}') \\ & + CH^3 + Dh(\mathbf{r})^3 + \dots \end{aligned}$$

Along the lines of Eq. (20), where we have written the most general expansion consistent with the governing symmetries, we further expand the interactions. For example, we write

$$\begin{aligned} \int d^d r' J(\mathbf{r}, \mathbf{r}') s(\mathbf{r}') &= \int d^d r' J(\mathbf{r}, \mathbf{r}') \left\{ s(\mathbf{r}) + \sum_{\alpha} (r_{\alpha} - r'_{\alpha}) \frac{\partial}{\partial r_{\alpha}} s(\mathbf{r}) \right. \\ &\quad \left. + \frac{1}{2!} \sum_{\alpha, \beta} (r_{\alpha} - r'_{\alpha}) (r_{\beta} - r'_{\beta}) \frac{\partial^2}{\partial r_{\beta} \partial r_{\alpha}} s(\mathbf{r}) + \dots \right\} \\ &= \left\{ \int d^d r' J(\mathbf{r}, \mathbf{r}') \right\} s(\mathbf{r}) + \sum_{\alpha} \left\{ \int d^d r' (r_{\alpha} - r'_{\alpha}) J(\mathbf{r}, \mathbf{r}') \right\} \frac{\partial}{\partial r_{\alpha}} s(\mathbf{r}) \\ &\quad + \frac{1}{2!} \sum_{\alpha, \beta} \left\{ \int d^d r' (r_{\alpha} - r'_{\alpha}) (r_{\beta} - r'_{\beta}) J(\mathbf{r}, \mathbf{r}') \right\} \frac{\partial^2}{\partial r_{\beta} \partial r_{\alpha}} s(\mathbf{r}) + \dots \end{aligned} \quad (20)$$

If the couplings are invariant under translations and rotations, then  $J(\mathbf{r}, \mathbf{r}') = J(|\mathbf{r} - \mathbf{r}'|)$ , the odd powers in Eq. (20) vanish and the even powers take a symmetric form, resulting in



$$\int d^d r' J(\mathbf{r}, \mathbf{r}') s(\mathbf{r}') = a s(\mathbf{r}) + b \nabla^2 s(\mathbf{r}) + \dots, \quad (21)$$

where  $a$  and  $b$  are numerical coefficients obtained from  $J$ . The derivative terms couple neighboring spins by hampering (or favoring, depending on the sign of the prefactors) spatial fluctuations. In their interplay with disorder effects, such short-range interactions introduce higher complications. By analogy with the driven disordered Ising model, we consider a mean-field approximation by substituting the derivative interactions with a uniform restoring force composed of  $\langle s \rangle$ ,  $\langle s \rangle^3$ ,  $H \langle s \rangle^2$ ,  $H^2 \langle s \rangle$ , etc. If a similar procedure is applied to the various terms in  $f_{\mathbf{r}}$ , we obtain

$$f_{\mathbf{r}} = a s(\mathbf{r}) + b' \langle s \rangle + A H + B h(\mathbf{r}) + c s(\mathbf{r})^3 + \left( \text{other terms, such as } \langle s \rangle^3, H s^2, h^2 s, \text{ or } H^3 \right). \quad (22)$$

To get a flavor of the construction and treatment of a phenomenological theory, rather than to examine the problem in full rigor, we abandon the “other terms” for now — we argue below that they do not change the critical properties. Furthermore, for ease of notation, we shall not drag along the many prefactors; the reader may either imagine them present or assume that they have been set to unity. Thus, our task is now to solve Eq. (18), which has been reduced to

$$s(\mathbf{r}) + \langle s \rangle - H + h(\mathbf{r}) + s(\mathbf{r})^3 = 0. \quad (23)$$

The prefactor of  $H$  has been set to  $-1$  so that  $s$  aligns along  $H$  at large values of the latter. This *stability condition* is imposed in addition to the various symmetries. In solving Eq. (23), we think of  $\langle s \rangle$  as a given function of  $H$ . If the resulting  $s(\mathbf{r})$  does not average to  $\langle s \rangle$ , our choice was not good, and we start over with a better guess for  $\langle s \rangle$ , until eventually the spatial average of  $s(\mathbf{r})$  is equal to  $\langle s \rangle$  for all  $H$ . In practice, Eq. (23) may be solved iteratively by reshuffling the terms, as

$$\begin{aligned} s(\mathbf{r}) &= -\langle s \rangle + H - h(\mathbf{r}) - s(\mathbf{r})^3 \\ &= -\langle s \rangle + H - h(\mathbf{r}) - [-\langle s \rangle + H - h(\mathbf{r})]^3 - \dots \end{aligned} \quad (24)$$

Clearly, performing the average over space or over disorder is equivalent, and the self-consistency condition results in

$$(3\sigma^2 - 2) \langle s \rangle + \langle s \rangle^3 = (3\sigma^2 - 1)H + (\text{higher-order terms}), \quad (25)$$

where  $\sigma^2 = \langle h^2 \rangle$ . For large disorders, the magnetization  $\langle s \rangle$  is a non-singular function of  $H$ . At a critical value  $\sigma^2 = 2/3 \equiv \sigma_c^2$ , however,  $\langle s \rangle \propto H^{1/3}$  and the response function diverges as

$$\chi = \left. \frac{\partial \langle s \rangle}{\partial H} \right|_{H \rightarrow 0} \sim H^{-2/3}, \quad (26)$$

reproducing the critical exponent of the driven disordered Ising model.

Let us return to the “other terms” neglected in Eq. (23), and argue that they do not modify the exponents. Indeed, any one of them either vanishes upon averaging ( $h^3$  for example) or is subleading in the limit  $H, \langle s \rangle \rightarrow 0$  (for example,  $H^2 s$  yields  $H^3$  and  $H^2 \langle s \rangle$  upon averaging). In a third possibility, the additional terms modify the prefactors in Eq. (25) (for example,  $h^2 s$  yields  $\sigma^2 \langle s \rangle$  upon averaging), but do not generate new types of terms. The symmetries are constraining enough to impose the cubic root behavior of the magnetization close to criticality. In a mean-field approach, in particular, where the system is reduced to a single degree of freedom, the exponents follow from an algebraic equation such as Eq. (25). This observation sheds some light on the (then quite cryptic) remark in Sec. II, that an exponent  $-1/2$  “is to be expected within a mean-field approach.” Without the reflection symmetry that we have assumed in the derivation of Eq. (25), quadratic terms would appear and clearly lead to an inverse square root divergence in the response function.

Another way to understand the decoupling that occurs in a mean-field theory and its essentially zero-dimensional nature (single degree of freedom) is obtained in a formulation closer to equilibrium statistical mechanics where the central objects are probability weights and partition functions. From rewriting Eq. (23) as

$$-h(\mathbf{r}) = s(\mathbf{r}) + \langle s \rangle - H + s(\mathbf{r})^3 \quad (27)$$

and the random field density

$$p(h) = \mathcal{N} e^{-\frac{h^2}{2\sigma^2}}, \quad (28)$$

where  $\mathcal{N}$  is a normalizing factor, the spin field is distributed according to

$$\rho(s(\mathbf{r})) = \mathcal{N} \exp \left[ -\frac{1}{2\sigma^2} (s(\mathbf{r}) + \langle s \rangle - H + s(\mathbf{r})^3)^2 \right] \times \|\text{Jacobian}\|. \quad (29)$$

Again, we require the self-consistency condition

$$\langle s \rangle = \int ds s \rho(s), \quad (30)$$

and the problem reduces to a zero dimensional one: finding the average of  $s$  at a single “site.” The right-hand-side of Eq. (30) may be evaluated by expanding the exponential in the super-quadratic terms of its argument and calculating Gaussian integrals.

In the absence of modulated interactions, the Jacobian is easily evaluated as  $1 + 3s$ . Beyond the mean-field picture, however, fluctuations matter regardless of their coupling to  $h$ , and the need for and use of a Jacobian becomes quite cumbersome. For a brief (and very superficial) discussion of richer theories, we return to the formulation of Eq. (23), whose analog for the case of short-range interactions reads

$$s(\mathbf{r}) + \nabla^2 s(\mathbf{r}) - H + h(\mathbf{r}) + s(\mathbf{r})^3 = 0. \quad (31)$$

How does the coupling between neighboring spins, expressed in the Laplacian term, modify the critical behavior? This question is best examined through the renormalization-group theory [24], which provides a systematic way to keep track of the role of each intervening term. Roughly speaking, it enables us to carry out an iterative solution (or averaging), similar to that of Eq. (24), in successive steps corresponding to progressively larger scales. Interestingly, it is found that the answer depends only on the dimension  $d$  of the system. Above six dimensions, a system described by Eq. (31) behaves just as the mean-field one of Eq. (23) [19,20], as far as critical exponents go. In some sense, it is bundled tightly enough so that a small push might move a lot. (Many hay stems are often dragged along when one is pulled out of a three-dimensional pile; this does not happen if the hay stems are laying on the two dimensional surface of a pond.) In  $d < 6 \equiv d_c$  (called “upper critical dimension”), the situation is far less trivial, and novel exponents emerge from the interplay of the Laplacian and random terms [19,20]. We might also expect intuitively that longer ranged interactions “more easily” lead to mean-field behavior and, indeed, they reduce the upper critical dimension. The case in which  $d_c < 3$  explains the trivial, mean-field-like exponents associated with some observed critical phenomena that, *a priori*, involve many complicated interactions.

In some instances, fluctuations bring about further surprises. A mean-field approximation somehow “homogenizes” the system, imposing a high degree of symmetry. Fluctuations might then break the latter into lower symmetries: a flat surface is invariant under any translation, whereas a periodically corrugated one is unchanged only under translations by the period’s multiples. New critical points then appear, corresponding to the new symmetries. This is exactly what happens in a system defined by the vectorial generalization of Eq. (23) [21], with the new degrees of freedom  $\vec{s}(\mathbf{r}) \in \mathfrak{R}^n$ . At the mean-field level, the critical properties correspond to a full rotational symmetry (in spin space). For short-range interactions, new critical points appear, associated with rotational invariance in subspaces of  $\mathfrak{R}^n$  [21].

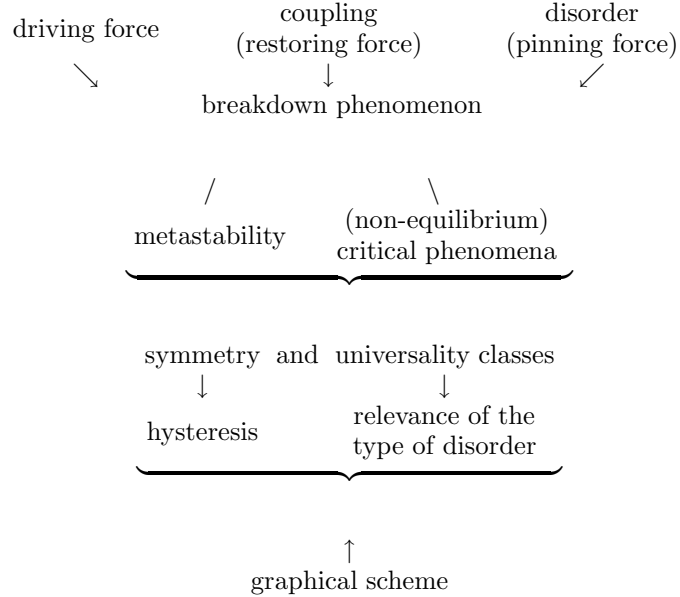
It is truly remarkable that we are able to make precise predictions based on such a general approach, without a definite model or “fundamental” understanding of the details. It is equally surprising that a complicated assembly of electrons and nuclei generates pure numbers, the critical exponents, which can be measured with great accuracy.

## VI. CONCLUSION

The models examined in Secs II–IV are probably less interesting for their own sake than for their illustrative power. Also, they provide motivation and inspiration for more complex, robust formulations closer to physical reality. This is especially true of simple models involving ubiquitous features such as driving forces, elastic interactions, and disorder. The breakdown of a disordered conductor under an applied current or voltage drop (often thought of as a jumping board to fracture problems) is yet another illustration. In a simple formulation [5], it may in fact be mapped to the driven disordered Ising model and the graphical scheme presented here is readily applicable to it.

The ability to solve such basic models serves as a first step toward the study of richer, more realistic physics. A class of problems akin to breakdown phenomena relates to the depinning and transport of elastic manifolds through disordered media [15,16]. The many variations on this paradigmatic theme include charge density waves [16], surface growth [25,15], contact lines [26,27,16], polymers [15], flux lines in superconductors [15,16], fractures [16], and earthquakes [16]. Another class of related examples pertains to social dilemmas, as illustrated by financial markets [28,29],

traffic flow, and internet congestion problems [30]. Given this wide range of interesting systems, it is worthwhile to acquire an elementary understanding and intuition from some simple related models. A rough “conceptual web” involved in the three examples we discussed in some detail is illustrated in the following diagram.



The main gap between our discussion and a more complete description of reality is the absence of any *dynamics* [31] in our formulation. It takes some time for an elevator rope to break, during which stress is redistributed. At a boarding gate, sitting people are watching, thinking, and deciding *while* an impatient passenger walks up to the line. A driven magnet responds with some delay, and different parts of the system are continually changing while they influence one another. By contrast, our formulation proposes algebraic equations to describe the system rather than equations of motion. In the spirit of effective theories, we can extend Eqs. (23) and (31) to include time dependences by letting  $s(\mathbf{r})$  depend explicitly on time and replacing the vanishing right-hand-side by a series such as

$$\alpha \frac{\partial}{\partial t} s(\mathbf{r}, t) + \beta \frac{\partial^2}{\partial t^2} s(\mathbf{r}, t) + \dots \quad (32)$$

This modification introduces correlations in time and leads to a wealth of results relating to fluctuations in time [31].

## ACKNOWLEDGMENTS

It is a pleasure to acknowledge Professor Mehran Kardar’s precious guidance and many interesting discussions. The author is also grateful to Paul de Sa, as well as to Sohrab Ismail-Beigi and Joel Moore, for commenting on the manuscript, and to the editors of the theme issue, Harvey Gould and Jan Tobochnik, for their careful review. This work was supported by the NSF through Grant No. DMR-98-05833.

- 
- [1] For a general introduction and review on conductor breakdown, fractures, and earthquakes, see B. K. Chakrabarti and L. G. Benguigui, *Statistical Physics of Fracture and Breakdown in Disordered Systems* (Clarendon Press, Oxford, 1997).
  - [2] F. T. Peirce, “Tensile tests for cotton yarns. V. – ‘The weakest link’, Theorems on the strength of long and composite specimens,” *J. Textile Inst.* **17**, T355–368 (1926).
  - [3] H. E. Daniels, “The statistical theory of the strength of bundles of threads. I,” *Proc. R. Soc. London A* **183**, 405–435 (1945).

- [4] R. da Silveira, “Comment on ‘tricritical behavior in rupture induced by disorder,’” *Phys. Rev. Lett.* **80**, 3157 (1998).
- [5] S. Zapperi, Purusattam Ray, H. E. Stanley, and A. Vespignani, “First-order transition in the breakdown of disordered media,” *Phys. Rev. Lett.* **78**, 1408–1411 (1997).
- [6] J. P. Sethna, K. Dahmen, S. Kartha, J. A. Krumhansl, B. W. Roberts, and J. D. Shore, “Hysteresis and hierarchies: dynamics of disorder-driven first-order phase transformations,” *Phys. Rev. Lett.* **70**, 3347–3350 (1993).
- [7] J. V. Andersen, D. Sornette, and K.-t Leung, “Tricritical behavior in rupture induced by disorder,” *Phys. Rev. Lett.* **78**, 2140–2143 (1997).
- [8] D. Sornette, “Mean-field solution of a block-spring model of earthquakes,” *J. Phys. I France* **2**, 2089–2096 (1992).
- [9] B. Q. Wu and P. L. Leath, “Failure probabilities and tough-brittle crossover of heterogeneous materials with continuous disorder,” preprint, cond-mat/9811044 and references therein.
- [10] A. Garciamartín, A. Guarino, L. Bellon, and S. Ciliberto, “Statistical properties of fracture precursors,” *Phys. Rev. Lett.* **79**, 3202–3205 (1997).
- [11] E. Ising, *Z. Physik* **31**, 253 (1925). For an introductory review, see Ref. 12, Chapters 14 and 15. For a more advanced treatment, see Ref. 13, Chapters 3 and 4.
- [12] K. Huang, *Statistical Mechanics* (John Wiley and Sons, New York, 1987).
- [13] G. Parisi, *Statistical Field Theory* (Addison-Wesley Publishing Company, Redwood City, CA, 1988).
- [14] For a review of the random-field Ising model, see T. Nattermann, “Theory of the random-field Ising model,” in *Spin Glasses and Random Fields*, ed. A. P. Young (World Scientific, Singapore, 1997), which can also be found under cond-mat/9705295.
- [15] For a review of non-equilibrium fluctuations of manifolds in random media and in particular polymers, flux lines, and interfaces, see M. Kardar, “Nonequilibrium dynamics of interfaces and lines,” *Phys. Rep.* **301**, 85–112 (1998) and references therein.
- [16] For a review of transport of manifolds in random media, and in particular charge density waves, flux lines, cracks and faults, see D. S. Fisher, “Collective transport in random media: from superconductors to earthquakes,” *Phys. Rep.* **301**, 113–150 (1998) and references therein.
- [17] T. Schneider and E. Pytte, “Random-field instability of the ferromagnetic state,” *Phys. Rev. B* **15**, 1519–1522 (1977).
- [18] A. Aharony, “Tricritical points in systems with random fields,” *Phys. Rev. B* **18**, 3318–3327 (1978).
- [19] K. Dahmen and J. P. Sethna, “Hysteresis loop critical exponents in  $6 - \epsilon$  dimensions,” *Phys. Rev. Lett.* **71**, 3222–3225 (1993).
- [20] K. Dahmen and J. P. Sethna, “Hysteresis, avalanches, and disorder-induced critical scaling: a renormalization-group approach,” *Phys. Rev. B* **53**, 14872–14905 (1996).
- [21] R. da Silveira and M. Kardar, “Critical hysteresis for  $n$ -component magnets,” *Phys. Rev. E* **59**, 1355–1367 (1999).
- [22] An effective theory for magnetic systems was first introduced in L. D. Landau, *Phys. Z. Sowjetunion* **11**, 26 (1937), reprinted in *Collected Papers of L. D. Landau*, ed. D. ter Haar (Pergamon, London, 1965), p. 193, and V. L. Ginzburg and L. D. Landau, *Zh. Eksp. Theor. Fiz.* **20**, 1064 (1950). For a review, see Ref. 23, Chapter 2 and Ref. 12, Chapter 17.
- [23] S.-K. Ma, *Modern Theory of Critical Phenomena* (Addison-Wesley Publishing Company, Reading, MA, 1976).
- [24] For an introduction to the renormalization-group theory, see Ref. 12, Chapter 18, Ref. 13, Chapters 7–9. Other good books on the subject include Ref. 23 and D. J. Amit, *Field Theory, the Renormalization Group, and Critical Phenomena* (World Scientific, Singapore, 1984), 2nd ed.
- [25] A.-L. Barabási and H. E. Stanley, *Fractal Concepts in Surface Growth* (Cambridge University Press, Cambridge, 1995).
- [26] P.-G. de Gennes, “Wetting: statics and dynamics,” *Rev. Mod. Phys.* **57**, 827–863 (1985).
- [27] D. Ertas and M. Kardar, “Critical dynamics of contact line depinning,” *Phys. Rev. E* **49**, R2532–2535 (1994).
- [28] B. B. Mandelbrot, *Fractals and Scaling in Finance: Discontinuity, Concentration, Risk* (Springer Verlag, 1997).
- [29] J.-P. Bouchaud and M. Potters, *Théorie des Risques Financiers* (Aléa Saclay, Paris, 1997); *Theory of Financial Risk*, to be published.
- [30] B. A. Huberman and R. M. Lukose, “Social dilemmas and internet congestion,” *Science* **277**, 535–537 (1997) and references therein.
- [31] For a review of dynamical critical phenomena, see P. C. Hohenberg and B. I. Halperin, “Theory of dynamical critical phenomena,” *Rev. Mod. Phys.* **49**, 435–479 (1977) and Ref. 23, Chapters 11–14.